Sea ice thickness retrieval from SMOS brightness temperatures during the Arctic freeze-up period

L. Kaleschke,[1] X. Tian-Kunze,[1] N. Maaß,[1] M. Mäkynen,[2] and M. Drusch[3]

[1] The Microwave Imaging Radiometer using Aperture Synthesis (MIRAS) on board the European Space Agency's (ESA) Soil Moisture and Ocean Salinity (SMOS) mission for the first time measures globally Earth's radiation at a frequency of 1.4 GHz (L-band). It had been hypothesized that L-band radiometry can be used to measure the sea ice thickness due to the large penetration depth in the sea ice medium. We demonstrate the potential of SMOS to derive the thickness of thin sea ice for the Arctic freeze-up period using a novel retrieval algorithm based on Level 1C brightness temperatures. The SMOS ice thickness product is compared with an ice growth model and independent sea ice thickness estimates from MODIS thermal infrared imagery. The ice thickness derived from SMOS is highly consistent with the temporal development of the growth simulation and agrees with the ice thickness from MODIS images with 10 cm standard deviation. The results confirm that SMOS can be used to retrieve sea ice thickness up to half a meter under ideal cold conditions with surface air temperatures below $-10°C$ and high-concentration sea ice coverage. **Citation:** Kaleschke, L., X. Tian-Kunze, N. Maaß, M. Mäkynen, and M. Drusch (2012), Sea ice thickness retrieval from SMOS brightness temperatures during the Arctic freeze-up period, *Geophys. Res. Lett.*, *39*, L05501, doi:10.1029/2012GL050916.

1. Introduction

[2] The ocean-atmosphere heat exchange is controlled by the sea ice thickness distribution in the polar oceans. Thin ice with a thickness of less than half a meter dominates the overall heat exchange and thus has a potential impact on weather and climate [*Maykut*, 1978]. Sea ice thickness can be inferred from Archimedes law and measurements of freeboard [*Laxon et al.*, 2003; *Kwok and Rothrock*, 2009]. However, the altimetric measurement results in large relative errors for thin ice [*Laxon et al.*, 2003]. Thickness of thin ice can be estimated from ice surface temperature using thermal infrared imagery but this technique is restricted to cold clear sky conditions and is strongly affected by fog and thin clouds [*Yu and Rothrock*, 1996]. Passive microwave radiometry at frequencies of 19 and 37 GHz (wavelength λ of 1.5 cm and 8 mm) has been used to estimate ice thickness. However, this microwave method is based on correlations between surface properties and thickness, valid only for ice

thicknesses less than 10–20 cm [*Martin et al.*, 2004; *Tamura and Ohshima*, 2011]. With ESA's Soil Moisture and Ocean Salinity (SMOS) mission, launched 2nd November 2009, and NASA's Aquarius mission, launched on 10th June 2011, there are two passive microwave sensors available that for the first time measure globally Earth's radiation at a frequency of 1.4 GHz (λ = 21 cm), the so-called L-band [*Kerr et al.*, 2010]. The potential of L-band radiometry for sea ice thickness retrieval has been demonstrated prior to the SMOS launch with airborne radiometric and electromagnetic induction (EM) measurements performed during the Pol-ICE Campaign 2007 over the Baltic sea ice [*Kaleschke et al.*, 2010]. However, a number of adverse circumstances prevented well-founded conclusions: firstly, the campaign was conducted under wet snow and ice conditions. Secondly, the spatial overlap between the L-band and EM-measurements was relatively small. Thirdly, the radiometer was not operating at its nominal performance and the EM data was potentially affected by the shallow bathymetry as well as sea ice ridging. Moreover, the depth for possible thickness retrieval under Arctic conditions could not be estimated as the campaign took place over low-salinity sea ice. Thus, the question remains if the L-band radiometric measurement of Arctic or Antarctic sea ice thickness is feasible and to what maximum the thickness can be retrieved.

[3] In this paper, we analyze SMOS brightness temperatures and the corresponding sea ice thickness retrieval for Arctic freeze-up period in fall 2010. The spatio-temporal ice thickness evolution is assessed with empirical estimations from the surface air temperature and from MODIS thermal imagery. The analysis also answer the question of maximum depth of the retrieval under ideal cold conditions for high-concentration Arctic sea ice.
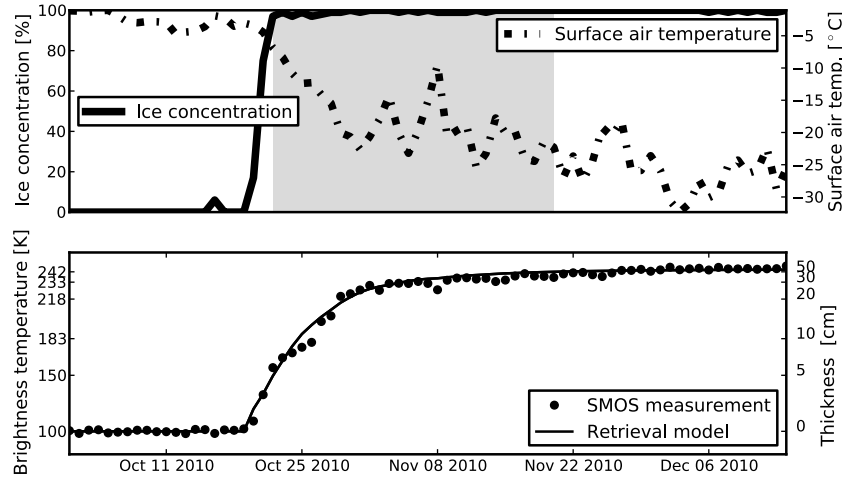
2. SMOS Data and Thickness Retrieval

[4] SMOS was launched in November 2009 and has been providing data for the scientific community since summer 2010 [*Mecklenburg et al.*, 2012]. It offers the capability of multi-angle multi-polarization measurements [*Kerr et al.*, 2010]. Based on the SMOS level 1C product, i.e., brightness temperatures at the top of the atmosphere, we compute the first Stokes parameter (intensity) as the mean of the vertical and horizontal component of the measured brightness temperatures. This parameter exhibits a strongly reduced angular dependency due to the fact that the positive and negative slope of the polarized components compensate each other. Therefore, data observed in the angular range of up to $\theta < 40°$ can be averaged over each individual location reducing the random errors introduced by the instrument. Moreover, usage of the first Stokes parameter

[1]Institut für Meereskunde, University of Hamburg, Hamburg, Germany.
[2]Finnish Meteorological Institute, Helsinki, Finland.
[3]ESTEC, ESA, Noordwijk, Netherlands.

Figure 1. (top) Time series of AMSR-E ice concentration and NCEP surface air temperature, and (bottom) SMOS observed and modeled brightness temperature with the corresponding ice thickness at 77.5°N, 137.5°E (indicated in Figure 3). The particular ice growth period discussed in the text is indicated in grey. The modeled brightness temperature is based on equation (2) and the ice thickness from Lebedev's growth parameterization.

avoids possible errors attributable to the ionospheric Faraday rotation that influences the polarization but not the intensity. Furthermore, the largest sensitivity concerning ice thickness and smallest atmospheric influence is also expected in nadir due to the minimum pathlength through ice and atmosphere, respectively. In addition, the highest horizontal resolution of about 35 km is obtained close to nadir. The resolution reduces to 45 km at the edges ($\theta = 40°$) of the ~1000 km wide swath. This scan configuration allows a complete daily coverage of the latitudes between 50° and 86°.

[5] SMOS measures in a protected frequency band to avoid unwanted anthropogenic signals. However, radio frequency interferences (RFI) are the largest error sources [*Mecklenburg et al.*, 2012] and RFI contaminated measurements are very difficult to correct. Localized RFI sources have a non-local impact on the whole field of view, called snapshot, since the synthetic aperture image reconstruction involves an inverse Fourier transformation [*Corbella et al.*, 2004]. Signals exceeding a threshold of 300 K are a clear indicator for RFI-occurrence and are taken as a flag for contaminated snapshots which are neglected subsequently.

[6] The observed brightness temperature T_{obs} depends on the fractional ice coverage, the temperatures of the sea T_{sea} and the ice T_{ice}, and their emissivities e_{water} and e_{ice}, respectively. In addition, the signal is slightly attenuated by the atmosphere and includes the reflected sky background and RFI. In the following we neglect these additional contributions and assume a spatially homogeneous ocean that is either ice free or 100% covered by sea ice. Thus, the observed brightness temperature over sea ice is given as
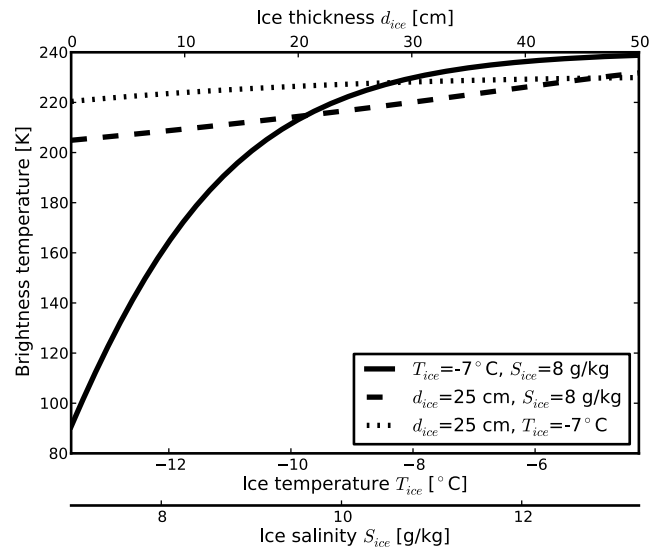
$$T_{\text{obs}} = e_{\text{ice}} T_{\text{ice}} \qquad (1)$$

By assuming a homogeneous dielectric-slab of thickness d_{ice} the emissivity $e_{\text{ice}}(\epsilon_{\text{ice}}, d_{\text{ice}})$ is calculated according to *Kaleschke et al.* [2010] with the parameterization of *Vant et al.* [1978] for the permittivity of sea ice $\epsilon_{\text{ice}}(V_b)$ as a function of the relative brine volume V_b. The relation of *Cox and Weeks* [1983] is used to determine the relative brine
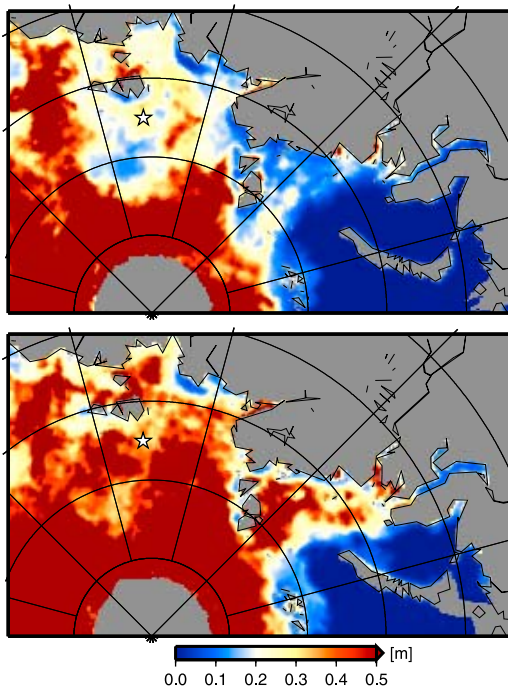
volume $V_b(T_{\text{ice}}, S_{\text{ice}})$ mainly as a function of bulk ice salinity S_{ice}, and temperature T_{ice}. A semi-empiric approximation for the incoherent solution of equation (1) is given by the following expression [*Kaleschke et al.*, 2010]

$$T_{\text{obs}} = T_1 - (T_1 - T_0) \exp(-\gamma d), \qquad (2)$$

with the brightness temperatures of open water $T_0(T_{\text{water}}, S_{\text{water}})$ and infinitely thick sea ice $T_1(T_{\text{ice}}, S_{\text{ice}})$, and an

Figure 2. Change of brightness temperature as a function of ice thickness, bulk ice temperature, and bulk salinity simulated using the model equation (1). In each case two parameters have been kept constant at an average value while the third parameter was varied. The variability represents the situation in the Laptev Sea during Oct 22 to Nov 20, 2010. Note that the present model includes neither the atmospheric and sky contributions nor a snow cover. Thus, the model underestimates the maximal observed brightness temperature T_1 by about 5 K.

Figure 3. Sea ice thickness in the Russian Arctic on (top) Nov 1 and (bottom) Nov 15 2010. The white star indicates the grid cell position for the time series analysis (Figure 1).

attenuation factor $\gamma(T_{\mathrm{ice}}, S_{\mathrm{ice}})$. We call the parameters T_0 and T_1 tie points analogous to the denomination used for ice concentration algorithms. Equation (2) can be inverted for the calculation of ice thickness from the observed brightness temperature. The maximum ice thickness $d_{\max}$ that can be retrieved for a given observational error δ is defined by the condition

$$d_{\max} = -\frac{1}{\gamma} \ln\left(\frac{\delta}{\Delta}\right), \tag{3}$$

with the measurement range $\Delta = T_1 - T_0$. The observational error δ is defined as the determination uncertainty of the tie point T_1. Thus, δ includes the measurement uncertainty as well as the geophysical uncertainty due to the variability of emissivity.

3. Results

[7] In order to demonstrate the algorithm, perform a preliminary verification and estimate the maximum thickness we first analysed data for a single grid point in the Laptev Sea at 77.5°N, 137.5°E. Figure 1 shows the corresponding time series of brightness temperature, ice concentration from AMSR-E [*Cavalieri et al.*, 2004], as well as surface air temperatures T_a from NCEP reanalysis [*Kalnay et al.*, 1996]. Before the first sea ice occurrence on about Oct 20, the observed brightness temperature was constant at $T_0 = 100.5 \pm 1$ K which defines the first tie point for the retrieval. Within very few days the ice cover changes from 0% to 100% accompanied by a decrease in air temperature and a monotonic increase in SMOS brightness temperature. After the ice concentration reaches 100%, the brightness

temperature continues to increase for about four weeks until about Nov 20. This particular sea ice growth period at about 100% concentration is highlighted in Figure 1. For the three weeks after Nov 22 the brightness temperature averages at $T_1 = 244.8 \pm 1.3$ K, marking the second tie point for thick first year ice.
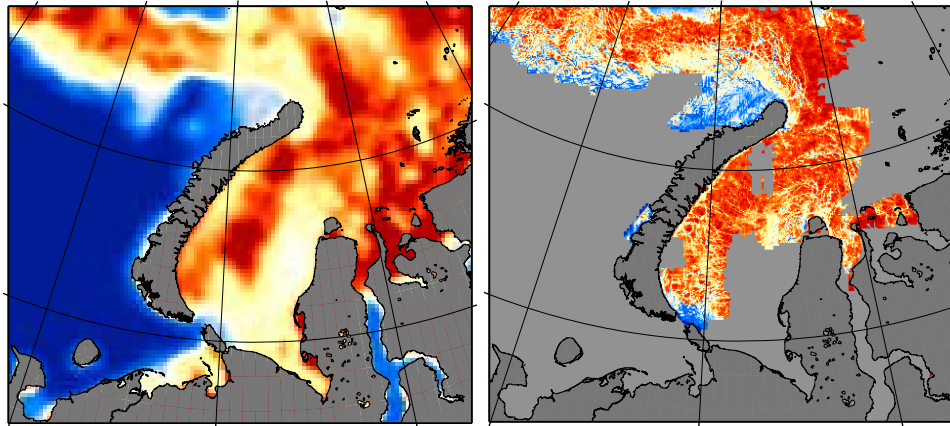
[8] Lebedev derived a parameterization for the sea ice thickness $d = 1.33\Theta^{0.58}$ [cm] as a function of the freezing-degree days $\Theta = \int(T_f - T_a)dt$, with the surface air temperature T_a and the freezing point of sea water $T_f \approx -1.9°C$ [*Maykut*, 1986]. This ice growth parameterization is well established [e.g., *Yu and Lindsay*, 2003], and used to obtain a first guess of the temporal thickness evolution with the surface air temperature as shown in Figure 1. Since sea ice development begins only when the complete mixed layer of the ocean is at or slightly below the freezing point of sea water, we constrain the timing of the freezing-degree day integration to the first occurrence of ice in corresponding AMSR-E ice concentration data. According to Lebedev's growth model, the thickness increases from about 5 cm to 50 cm during the four week period from October 20 to November 20.

[9] Although the simulated ice thickness is completely independent from the SMOS brightness temperature we cannot conclude from a correlation that the increase of brightness temperature is solely caused by the increase of ice thickness. Therefore, we use the brightness temperature model equation (1) to distinguish between the influence of ice thickness, bulk ice temperature and salinity on the brightness temperature. The period of sea ice growth indicated in Figure 1 serves as a baseline to estimate the variability of ice thickness, bulk ice temperature and salinity. The bulk ice temperature is estimated as an average of the surface air temperature and the ice bottom temperature at the freezing point of sea water. The variability of bulk salinity is derived from the minimum and maximum ice thickness according to *Cox and Weeks* [1974]. We estimate a bulk ice temperature of $T = -7°C$ and a salinity of $S = 8$ g/kg as representative averages for the baseline growth period. The sensitivity analysis shown in Figure 2 confirms that ice thickness is the dominating factor controlling brightness temperature.

[10] We obtain $\gamma(T_{\mathrm{ice}} = -7°C, S_{\mathrm{ice}} = 8 \text{ g/kg}) = 8.5 \text{ m}^{-1}$ by a least-squares optimization using the two models equations (1) and (2). For the following we assume the parameter γ as constant in time and space. With the two tie points T_0 and T_1 as obtained from the time series of Figure 1, equation (2) is used to calculate the brightness temperature as a function of the simulated ice thickness. Vice versa, the inversion of equation (2) can be used to retrieve the ice thickness from the observed SMOS brightness temperatures. Equation (3) with $\delta = 1.3$ K predicts a maximum depth $d_{\max} = 0.55$ m.

[11] Figure 1 shows the simulated and the retrieved SMOS ice thickness. The correlation is $R^2 = 0.97$ when excluding the ice thickness values above 0.5 m. There is no significant correlation for values above $d > 0.5$ m in agreement with the previous prediction. The root mean square deviation between the SMOS retrieval and the freezing-degree day thicknesses is 4 cm with a negative bias of 2 cm.

[12] Using the retrieval parameters T_0, T_1, and γ as given above we have been calculating daily ice thickness maps for

Figure 4. Sea ice thickness in the Kara Sea derived from (left) SMOS and (right) MODIS on Dec 26, 2010. For color scale see Figure 3.

the freeze-up period in 2010. Figure 3 shows two examples for the ice thickness retrieved from SMOS for the Eastern Arctic where the contamination through RFI is small. The thickness maps provide many details such as the location of remaining thick ice that survived summer, as well as the ice growth between Nov 1 and Nov 15.

[13] For the assessment of the spatial thickness distribution we estimate the thin level ice thickness for the Kara Sea from MODIS nighttime data by using the surface heat balance equation [*Yu and Rothrock*, 1996]. The external forcing data for solving the surface heat balance was obtained from a numerical weather prediction (NWP) model HIRLAM (HIgh-Resolution Limited Area Model) [*Källen*, 1996; *Undén et al.*, 2002]. As a limited area model, HIRLAM requires lateral boundary conditions from global/hemispheric model, provided here by the European Centre for Medium Range Weather Forecasting (ECMWF). The sea ice concentration input for HIRLAM was based on the ECMWF operational sea surface temperature analysis. The HIRLAM model grid spacing was 20 km. Cloud masking of MODIS data was conducted using three cloud tests based on *Frey et al.* [2008] and manual methods. The MODIS sea ice surface temperature was calculated as by *Hall et al.* [2004]. On the average the ice thickness uncertainty is around 40% when the ice thickness 10–30 cm and increases to 50% when the thickness is 50 cm. The maximum reliable ice thickness is around 40–50 cm, depending on air temperature. Figure 4 shows the comparison of ice thickness derived from SMOS and MODIS in the Kara Sea on Dec 26, 2010. The MODIS ice thicknesses have been averaged on the SMOS grid with 12.5 km × 12.5 km spacing. The root mean square deviation between the SMOS and the MODIS retrieval is 10 cm with a negative bias of 2 cm. The pixel-by-pixel correlation is $R^2 = 0.5$.

4. Discussion and Conclusion

[14] Ground-truth measurements of sea ice thickness are sparse. Therefore, we use indirect but independent estimations of ice thickness to demonstrate the validity of the SMOS sea ice thickness retrieval method as proposed by *Kaleschke et al.* [2010]. The time series provides clear evidence for a strong correlation between SMOS brightness temperature and sea ice thickness. The causality of the relation is demonstrated through a sensitivity analysis by using a dielectric sea ice model to simulate the brightness temperature as a function of ice thickness, temperature, and salinity.

[15] The assumption of constant retrieval parameters and a closed ice cover are strong simplifications but seem to be reasonable for surface air temperatures below −10°C and when intermediate ice concentrations are only a transient phenomenon. An independent verification with ice thickness derived from MODIS further confirms the validity and consistency of the assumptions. Thus, for the first prototype of a retrieval algorithm we avoid the necessity of using auxiliary data and use constant retrieval parameters that are selected to represent average freeze-up conditions.

[16] In general, the brightness temperature is a function of ice concentration, ice temperature, and salinity, as well as the snow cover. Changes in ice concentration and ice temperature could cause significant errors. A snow cover could also change the ice temperature due to its thermal insulation and thus would have a longer-lasting effect than fluctuation of the atmospheric temperature. The bulk ice salinity decreases with time but we do not expect fluctuations such as for the ice temperature. Changes in surface roughness cannot be investigated with our model since it assumes a specular surface. Thus, several retrieval uncertainties remain that should be considered in future studies.

[17] Despite these uncertainties our analysis provides clear evidence for a maximum of the retrievable ice thickness $d_{max} \approx 0.5$ m. SMOS obtains daily coverage of the polar regions with a resolution of about 35 km × 35 km which is suitable for several applications of a sea ice thickness product. We expect the greatest benefit during the cold freeze-up period in Autumn when extensive areas of thin sea ice control the ocean-atmosphere heat exchange, which is important for weather and climate, as well as for operational marine applications.

[19] The Editor thanks two anonymous reviewers for their assistance in evaluating this paper.

References

Cox, G., and W. Weeks (1974), Salinity variations in sea ice, *J. Glaciol.*, *13*, 109–120.

Cox, G., and W. Weeks (1983), Equations for determining the gas and brine volumes in sea-ice samples, *J. Glaciol.*, *29*, 306–316.

Cavalieri, D., T. Markus, and J. Comiso (2004), AMSR-E/Aqua daily L3 12.5 km brightness temperature, sea ice concentration, and snow depth polar grids V002, digital media, Natl. Snow and Ice Data Cent., Boulder, Colo.

Corbella, I., N. Duffo, M. Vall-llossera, A. Camps, and F. Torres (2004), The visibility function in interferometric aperture synthesis radiometry, *IEEE Trans. Geosci. Remote Sens.*, *42*(8), 1677–1682.

Frey, R. A., S. A. Ackerman, Y. Liu, K. I. Strabala, H. Zhang, J. R. Key, and X. Wang (2008), Cloud detection with MODIS. Part I: Improvements in the MODIS cloud mask for collection 5, *J. Atmos. Oceanic Technol.*, *25*, 1057–1072.

Hall, D. K., J. R. Key, K. A. Casey, G. A. Riggs, and D. J. Cavalieri (2004), Sea ice surface temperature product from MODIS, *IEEE Trans. Geosci. Remote Sens.*, *42*(5), 1076–1087.

Kaleschke, L., N. Maaß, C. Haas, S. Heygster, and R. Tonboe (2010), A sea-ice thickness retrieval model for 1.4 GHz radiometry and application to airborne measurements over low salinity sea-ice, *Cryosphere*, *4*, 583–592, doi:10.5194/tc-4-583-2010.

Källen, E. (1996), *HIRLAM Documentation Manual, System 2.5*, 178 pp., Swed. Meteorol. and Hydrol. Inst., Norrköping, Sweden.

Kalnay, E., et al. (1996), The NCEP/NCAR 40-year reanalysis project, *Bull. Am. Meteorol. Soc.*, *77*, 437–471.

Kerr, Y. H., et al. (2010), The SMOS Mission: New tool for monitoring key elements of the global water cycle, *Proc. IEEE*, *98*(5), 666–687.

Kwok, R., and D. A. Rothrock (2009), Decline in Arctic sea ice thickness from submarine and ICESat records: 1958–2008, *Geophys. Res. Lett.*, *36*, L15501, doi:10.1029/2009GL039035.

Laxon, S., N. Peacock, and D. Smith (2003), High interannual variability of sea ice thickness in the Arctic region, *Nature*, *425*, 947–949, doi:10.1038/nature02050.

Martin, S., R. Drucker, R. Kwok, and B. Holt (2004), Estimation of the thin ice thickness and heat flux for the Chukchi Sea Alaskan coast polynya from Special Sensor Microwave/Imager data, 1990–2001, *J. Geophys. Res.*, *109*, C10012, doi:10.1029/2004JC002428.

Maykut, G. A. (1978), Energy exchange over young sea-ice in the central Arctic, *J. Geophys. Res.*, *83*, 3646–3658.

Maykut, G. A. (1986), The surface heat and mass balance, in *Geophysics of Sea Ice*, edited by N. Untersteiner, pp. 395–463, Plenum, New York.

Mecklenburg, S., et al. (2012), ESA's Soil Moisture and Ocean Salinity mission: Mission performance and operations, *IEEE Trans. Geosci. Remote Sens.*, in press.

Tamura, T., and K. I. Ohshima (2011), Mapping of sea ice production in the Arctic coastal polynyas, *J. Geophys. Res.*, *116*, C07030, doi:10.1029/2010JC006586.

Undén, P., et al. (2002), *HIRLAM-5 Scientific Documentation*, 144 pp., Swed. Meteorol. and Hydrol. Inst., Norrköping, Sweden.

Vant, M., R. Ramseier, and V. Makios (1978), The complex-dielectric constant of sea ice at frequencies in the range 0.1–40 GHz, *J. Appl. Phys.*, *49*, 1264–1280.

Yu, Y., and R. W. Lindsay (2003), Comparison of thin ice thickness distributions derived from RADARSAT Geophysical Processor System and advanced very high resolution radiometer data sets, *J. Geophys. Res.*, *108*(C12), 3387, doi:10.1029/2002JC001319.

Yu, Y., and D. A. Rothrock (1996), Thin ice thickness from satellite thermal imagery, *J. Geophys. Res.*, *101*, 25,753–25,766, doi:10.1029/96JC02242.

M. Drusch, ESTEC, ESA, Keplerlaan 1, NL-2201 AZ Noordwijk, Netherlands.

L. Kaleschke, N. Maaß, and X. Tian-Kunze, Institut für Meereskunde, University of Hamburg, Bundesstraße 53, D-20146 Hamburg, Germany. (lars.kaleschke@zmaw.de)

M. Mäkynen, Finnish Meteorological Institute, Erik Palmenin aukio 1, FI-00101 Helsinki, Finland.